HHS Public Access

Author manuscript

Brain Stimul. Author manuscript; available in PMC 2022 February 28.

Published in final edited form as:

Brain Stimul. 2021 ; 14(3): 703–709. doi:10.1016/j.brs.2021.04.010.

Targeting location relates to treatment response in active but not sham rTMS stimulation

A.C. Rosen[a,b,*], **J.V. Bhat**[a,c], **V.A. Cardenas**[a], **T.J. Ehrlich**[a,d], **A.M. Horwege**[a], **D.H. Mathalon**[e,f], **B.J. Roach**[e,g], **G.H. Glover**[h], **B.W. Badran**[i], **S.D. Forman**[j,k], **M.S. George**[i,l], **M.E. Thase**[m,n], **D. Yurgelun-Todd**[o,p], **M.E. Sughrue**[q,r], **S.P Doyen**[q], **P.J. Nicholas**[q], **J.C. Scott**[m,n], **L. Tian**[s], **J.A. Yesavage**[a,b]

[a]Veterans Affairs Palo Alto Health Care System, Palo Alto, CA, USA

[b]Department of Psychiatry, Stanford University, Stanford, CA, 94305, USA

[c]Palo Alto Veterans Institute for Research, Palo Alto, CA, 94304, USA

[d]University of Michigan, Ann Arbor, USA

[e]Mental Health Service, San Francisco Veterans Affairs Health Care System, University of California, San Francisco, CA, USA

[f]Department of Psychiatry and Behavioral Sciences, University of California, San Francisco, CA, USA

[g]Northern California Institute for Research and Education, San Francisco Veterans Affairs Medical Center, University of California, San Francisco, CA, USA

[h]Department of Radiology, Stanford University, Stanford, CA, USA

[i]Brain Stimulation Division, Department of Psychiatry, Medical University of South Carolina, Charleston, SC, USA

[j]Department of Veterans Affairs, VA Pittsburgh Healthcare System, Pittsburgh, PA, USA

[k]Western Psychiatric Institute and Clinic, University of Pittsburgh School of Medicine, Pittsburgh, PA, USA

[l]Ralph H. Johnson VA Medical Center, Charleston, SC, USA

[*]Corresponding author. Palo Alto VAHCS; 3801 Miranda Ave (151Y), Palo Alto, CA, 94304-1207, USA. rosena@stanford.edu (A.C. Rosen).

Author contributions

Allyson Rosen: Conceptualization, Methodology, Formal Analysis, Writing − Original Draft, Supervision, Project Administration, Funding Acquisition; **J.V. Bhat**: Software, Validation, Formal analysis, Writing − Original Draft, Visualization, Project Administration; **Valerie Cardenas**: Conceptualization, Software, Formal analysis, Visualization, Writing − Original Draft; **Tobin Ehrlich**: Software, Formal analysis, Conceptualization; **Andrea Horwege**: Project administration; **Daniel Mathalon**: Conceptualization, Formal analysis, Resources, Investigation; **Brian Roach**: Conceptualization, Formal analysis, Resources, Investigation; **Gary Glover**: Resources, Investigation; **Bashar Badran**: Resources, Investigation; **Steven Forman**: Resources, Investigation; **Mark George**: Conceptualization, Resources, Investigation; **Michael Thase**: Resources, Investigation; **Deborah Yurgelun-Todd**: Resources, Investigation; **Michael Sughrue**: Software, Formal Analysis; **Stephane Doyen**: Software, Formal Analysis; **Peter Nicholas**: Software, Formal Analysis; **J. Cobb Scott**: Resources, Investigation; **Lu Tian**: Formal analysis; **Jerome Yesavage**: Resources, Conceptualization, Investigation.

Appendix A. Supplementary data

Supplementary data to this article can be found online at https://doi.org/10.1016/j.brs.2021.04.010.

[m]VISN4 Mental Illness Research, Education, and Clinical Center at the Corporal Michael J. Crescenz VA Medical Center, Philadelphia, PA, 19104, USA

[n]Department of Psychiatry, Perelman School of Medicine, University of Pennsylvania, Philadelphia, PA, USA

[o]Rocky Mountain Network Mental Illness Research Education and Clinical Centers (VISN 19), VA Salt Lake City Health Care System, Salt Lake City, UT, USA

[p]Department of Psychiatry, University of Utah School of Medicine, Salt Lake City, UT, USA

[q]Omniscient Neurotechnologies, Sydney, Australia

[r]Prince of Wales Hospital, Randwick, NSW, Australia

[s]Department of Biomedical Data Science, Stanford University School of Medicine, Stanford, CA, USA

Abstract

Background: Precise targeting of brain functional networks is believed critical for treatment efficacy of rTMS (repetitive pulse transcranial magnetic stimulation) in treatment resistant major depression.

Objective: To use imaging data from a “failed” clinical trial of rTMS in Veterans to test whether treatment response was associated with rTMS coil location in active but not sham stimulation, and compare fMRI functional connectivity between those stimulation locations.

Methods: An imaging substudy of 49 Veterans (mean age, 56 years; range, 27e78 years; 39 male) from a randomized, sham-controlled, double-blinded clinical trial of rTMS treatment, grouping participants by clinical response, followed by group comparisons of treatment locations identified by individualized fiducial markers on structural MRI and resting state fMRI derived networks.

Results: The average stimulation location for responders versus nonresponders differed in the active but not in the sham condition ($P = .02$). The average responder location derived from the active condition showed significant negative functional connectivity with the subgenual cingulate ($P < .001$) while the nonresponder location did not ($P = .17$), a finding replicated in independent cohorts of 84 depressed and 35 neurotypical participants. The responder and nonresponder stimulation locations evoked different seed based networks (FDR corrected clusters, all $P < .03$), revealing additional brain regions related to rTMS treatment outcome.

Conclusion: These results provide evidence from a randomized controlled trial that clinical response to rTMS is related to accuracy in targeting the region within DLPFC that is negatively correlated with subgenual cingulate. These results support the validity of a neuro-functionally informed rTMS therapy target in Veterans.

Keywords

rTMS; Resting-state fMRI networks; Depression; Subgenual cingulate; Targeting; Dorsolateral prefrontal cortex

Introduction

Repetitive pulse transcranial magnetic stimulation (rTMS) of the dorsolateral prefrontal cortex (DLPFC) is an important therapy option for patients with treatment resistant major depression (TRMD) [1,2], although success varies [3−5]. Whereas depression likely involves multiple brain regions [6], the DLPFC is an accessible target for noninvasive brain stimulation treatment of TRMD due to its location near the scalp. In traditional clinical rTMS, the treatment location was identified based on landmarks on the scalp. Variations in patient head size and other factors led to stimulation of brain regions other than the DLPFC, thus affecting the efficacy of rTMS [3,4]. Early structural MRI studies attributed poor response to mistargeting in Brodmann's Areas (BA) 6 and 8, premotor regions [3−5]. More recent resting state fMRI studies showed that stimulation in regions with the strongest negative correlation (anticorrelation) with the subgenual cingulate [7−11] was related to greater Hamilton Depression Rating Scale (HAMD) improvements, suggesting that depression response is due to both direct DLPFC and downstream modulation of connected brain regions [12,13]. The location of rTMS stimulation is also related to improvement in dysphoric depression symptoms vs. anxiosomatic symptoms [14].

Given FDA approval of rTMS therapy for patients with TRMD and wide availability of the treatment, a moderately sized, sham-controlled rTMS study, even one with a neuroimaging component, faces challenges in recruitment of TRMD patients. Our recent multi-site, randomized, sham-controlled, double blind, rTMS study in Veterans [15,16] is thus particularly valuable. In this study, treaters identified a place on the scalp where TMS evokes a thumb twitch and positioned stimulation 6 cm toward the front of the head, a DLPFC-targeting variant of a popular clinical standard [1,2]. We demonstrated that there was no significant advantage of active rTMS (40.7% remission) over sham stimulation (37.4% remission). One interpretation is that rTMS benefit in Veterans is largely a placebo response [17]. We propose that mistargeting in the active condition reduced our response rate such that the benefit compared to sham stimulation was undetected.

This imaging study tested whether variations in targeting precision contributed to the failure to find an advantage over sham treatment. We hypothesized that in the active condition only, the average stimulation location of patients who respond to therapy differed from the average stimulation location of those who failed to respond (Hypothesis 1). Based on a mechanistic model of rTMS response [8−10], we further hypothesized that in the active condition, the fMRI time series within a subgenual cingulate region of interest (ROI) would be anticorrelated with the fMRI time series within an ROI centered at the stimulation location of the responders (defined as patients with > 50% change on the HAMD), and not with the ROI centered at the nonresponder stimulation location (Hypothesis 2). We also undertook an analysis of seed voxel-based functional connectivity, defined as the correlation between fMRI timecourses, to compare the networks that include seeds at the average active responder and nonresponder locations. We hypothesized that these seeds would be functionally connected with distinct brain networks (Hypothesis 3).

Methods and materials

Participants

Of the 342 patients assessed for eligibility in the original study, 164 were randomized to the larger sham-controlled clinical trial of rTMS (ClinicalTrials.gov ID: NCT01191333). Forty-nine Veterans with TRMD from the six centers with 3T MRIs were recruited and completed resting-state fMRI for this imaging sub-study. This study was approved by the Veterans Administration Central Institutional Review Board and the Research and Development Committee of the Veterans Affairs Palo Alto Health Care System. Participants signed an informed consent document and were paid for their participation in the study. Table 1 shows basic demographic information of the subgroup and original study; see previous publications for full inclusion and exclusion criteria [15,16].

Procedures

Sham and active transcranial magnetic stimulation therapy—The published stimulation protocol [15,16] is described in the Supplement (eMethods: TMS Details). Briefly, the rTMS device was a MagPro R30 stimulator with a Cool-B65-A/P coil (MagVenture, Farum, Denmark). This coil was enabled with an integrated sham mechanism that kept the entire site blinded to patient treatment assignment. Both active and sham conditions received transcutaneous electrical nerve stimulation on the forehead to simulate muscle contractions induced by stimulation of the frontal lobe. Patients listened to simulated stimulator noise through earphones. Stimulation was delivered 6 cm anterior to the motor hot spot (eMethods: Motor Hot Spot and Threshold/Dosage) with the coil oriented 45° relative to midline with the coil handle pointing posterior to the patient and lateral (i.e. away from midline). Each patient had a cloth cap marked with the treatment location (MagVenture, Farum, Denmark) for re-use by treaters to consistently position the treatment coil. RTMS treatment (10 Hz frequency, 4 s on, 10 s off, 120% motor threshold, 4000 pulses/session, 25 min per session) was delivered daily in blocks of 5 for a minimum of 20 sessions (80,000 pulses) and a maximum of 30 sessions (120,000 pulses) depending on whether the patient reached remission (24 item Hamilton Rating Scale for Depression score<11).

Clinical depression outcome measure—The primary efficacy outcome was clinical response (50% decline from Baseline) over the acute treatment phase on the 24-item HAMD (HAMD24). Patients were classified as responders or non-responders on this basis and further subdivided by treatment condition (active, sham).

MRI acquisition—Structural MRI and resting state fMRI were collected (eMethods: MRI Acquisition) while patients wore a treatment cap with a fiducial marker (eMethods: Fiducial Marker Protocol) identifying the rTMS treatment location, thus enabling identification of the underlying brain location stimulated. Imaging occurred prior to therapy-onset for 72% of patients receiving active rTMS; the remainder were imaged long after rTMS treatment ceased (minimum 259 days, average 19 months) to avoid the direct effects of brain stimulation therapy on fMRI.

MRI analysis

Identifying the Representative Brain Stimulation Locations (Rlocations) for Each Condition.: For each patient, the treatment location identified by the fiducial marker was projected to the underlying brain surface using MR image guidance software (Brainsight, Rogue Research, Montreal, CA). A different method of projection to the cortex (O8t, Omniscient, Sydney, Australia) was used to check the consistency of localization, and locations were labeled using an atlas derived from the HCP (Human Connectome Project) [18]. FSL routines [19] registered these cortical locations into MNI standard space (eMethods: Identifying Representative Brain Locations); these patient-specific locations were used to test Hypothesis 1. For each of the four groups (active stimulation responder, active stimulation nonresponder, sham stimulation responder, sham stimulation nonresponder) we computed the centroid of these stimulation locations to derive representative locations (hereafter referred to as Rlocations) in MNI coordinates and also estimated the spatial dispersion of treatment locations (eMethods: Dispersion of rTMS Treatment Locations). Rlocations were labeled using several atlases and used to test Hypotheses 2 and 3.

Hypothesis 1.

Responder and Nonresponder Rlocations are different: We used statistical testing by permutation [20] to build the distribution of distance between stimulation centroids by assigning patients to one of two groups and calculating the distance between the stimulation centroids, then repeating the process for all combinations of group assignment. Separate distributions were built for the active and sham conditions. If response is related to stimulation location, then the distances between the responder and nonresponder Rlocations should be in the upper 5% of the corresponding distribution (eMethods for details).

Resting State fMRI Connectivity Analysis.: Resting state fMRI analysis was performed in CONN [21,22]. After preprocessing (eMethods: Preprocessing) we tested:

Hypothesis 2.

Responder Rlocation is anticorrelated with Subgenual Cingulate, Nonresponder Rlocation is not. (eMethods for details).: Anticorrelations (converted to z-scores using the Fisher transformation) between an a priori defined subgenual cingulate ROI with MNI coordinates (6, 16, −10) and ROIs at the two active stimulation Rlocations were calculated for each of the 49 patients, and also in an independent sample of 84 TRMD patients and 35 neurotypical controls [23] (Table S1) to assess generalizability. These values were entered into a two-tailed *t*-test comparing anticorrelation values against a null hypothesis of zero (Statistica Version 13) with a Bonferroni-adjusted alpha level of 0.025 (0.05/2), and a paired *t*-test comparing anticorrelation between Rlocations.

Hypothesis 3.

Responder and Nonresponder Rlocations evoke distinct functional networks (eMethods for details).: To test the hypothesis that the locations identified by the responders and nonresponders in the active condition would evoke distinct networks, voxel-wise seed-based

functional connectivity maps were generated from each of the Rlocations. Difference maps were generated to compare networks.

Results

Clinical response

One patient who underwent MRI dropped out prior to therapy; for the remaining 48 patients, five failed to complete therapy. One of these 43 patients with treatment response had inaccurately placed MRI fiducials, leaving 42 patients contributing to the Rlocations (Figure S2). All 49 patients were retained for imaging analysis, as illustrated by Figure S1 in the supplement. The number of responders and nonresponders failed to differ between the active and sham conditions (X^2 [2, N = 48] = .614, P = .74). At the end of treatment, 33 patients with treatment response results completed surveys guessing their treatment assignment (Table S2). No evidence of a significant relationship between each patient's guess of treatment group assignment and their response status was observed (X^2 [1, N = 33] = 0.25, P = .61), indicating the subject's expectation of benefit was unrelated to response.

Imaging results

Representative Brain Stimulation Locations (Rlocations)—Fig. 1a shows the active stimulation locations on a standard brain, with yellow denoting responders and blue denoting non-responders. The Rlocations for each of the four groups and the numbers of participants from which they were derived follow: active-responder = (−42,34,38; N = 12); active-nonresponder = (−34,30,46; N = 6); sham-responder = (−38,36,34; N = 15); sham-nonresponder = (−42,38,34; N = 9). In Fig. 1b, the Rlocations are displayed using yellow/blue for responders/nonresponders and shape indicating condition (sphere = active, cube = sham). The active-nonresponder location was the most distinctly different from the other three conditions.

Hypothesis 1: Responder and Nonresponder Rlocations are different—The distance between the active-responder and active-nonresponder Rlocations was 16.5 mm, significantly farther apart than would be expected if response were not related to stimulation location (P = .02). The distance between the sham-responder and sham-nonresponder Rlocations was 4.5 mm, suggesting that response due to sham stimulation was not related to stimulation location (P = .73).

Atlas labeling at rlocations—Table 2 summarizes the anatomical regions and networks targeted by the Rlocations [18,24−26]. As shown, all Rlocations target DLPFC (green overlay, Fig. 1b) and frontoparietal (Fig. 1c) or salience/ventral attention networks except the active nonresponder Rlocation, which targets 8Av (red overlay, Fig. 1b) and the default mode network (Fig. 1c). Using O8t, 33% of active responders received stimulation in BA 8 and 67% in BA 9 or 46, consistent with the active RLocation label.

Hypothesis 2: Responder Rlocation is anticorrelated with subgenual cingulate, Nonresponder Rlocation is not—The average anticorrelation between the subgenual cingulate and the ROI at the active-nonresponder RLocation was not significantly

different from zero (0.03 ± 0.14, P = .17). Subgenual cingulate anticorrelation with the active-responder ROI was less than zero (−0.12 ± 0.15, P < .001) and significantly smaller than the anticorrelation with the nonresponder Rlocation (P < .001). This pattern of subgenual cingulate anticorrelation with the responder but not nonresponder seed was replicated in an independent sample (see eResults: Anticorrelation of Rlocations with Subgenual Seed Region in Independent Sample, Table S3).

Hypothesis 3: Responder and Nonresponder Rlocations evoke distinct functional networks—Multiple frontal and parietal regions in both hemispheres including the insula and the dorsal and ventral prefrontal cortex were more strongly connected to the responder Rlocation, with average connectivity with the responder seed higher by 0.20−0.43 compared to the nonresponder seed (Fig. 2, Table 3). A mask of these regions had the highest dice overlap [27] with the HCP salience network. The posterior cingulate, middle frontal gyrus (BA 9), angular gyrus (BA 39) and ventral frontal regions (BA 10) were more strongly connected to the nonresponder Rlocation, with average connectivity with the nonresponder seed higher by 0.26e0.39. A mask of these regions had the highest dice overlap with the HCP default mode network.

Discussion

This study leveraged the variability in position introduced by scalp-based targeting to demonstrate that patients that responded on the HAMD24 received active rTMS in DLPFC on average, in contrast to nonresponders that received targeted stimulation in area 8Av on average, as defined by modern multimodal and functional connectivity derived atlases [18,25]. Furthermore, clinical response to rTMS was related to targeting location in active stimulation only, as demonstrated by the spatial segregation of responder and nonresponder Rlocations in the active and not the sham condition. These results highlight the importance of studying focal brain targeting accuracy in clinical treatment and trials of rTMS. We used resting-state functional imaging to show that the subgenual cingulate was significantly anticorrelated with the active responder Rlocation in contrast to the nonresponder Rlocation. When examining whole-brain connectivity of seed-based networks derived from the Rlocations of active responders vs. active nonresponders, the responder Rlocation showed greater connectivity in multiple nodes of the salience and frontal-parietal control networks [28]. In contrast, the nonresponder Rlocation had greater connectivity in regions that are part of the default mode network [29]. This result reinforces the hypothesis that functionally distinct networks were modulated in responders and nonresponders receiving active stimulation.

The primary aim of this study was to test whether variations in the scalp-landmark based targeting method used in CSP556 contributed to the failure to find an advantage over sham treatment. Because early failures of rTMS using the 5 cm rule were hypothesized to be due to stimulation in BA 6, a premotor region, CSP556 used the 6 cm rule hoping to target anterior to BA 6. Despite careful application of the 6 cm rule, our imaging substudy observed variability in the scalp and underlying brain regions targeted (as shown in Fig. 1). Comparison of the stimulation sites with anatomical atlases [18,24] showed that CSP556 successfully avoided BA 6. While one-third of our responders were stimulated in BA 8,

consistent with a previous study reporting that stimulation in BA 8 led to remission in 28% of patients [4], our nonresponder results suggest that the heterogeneity within the large cytoarchitectonically defined BA 8 (that led to a newer atlas that subdivides Brodmann areas [18]) has clinical implications. Specifically, we observed that most of the patients receiving stimulation in area 8Av and the DMN were nonresponders. Scalp-based targeting based on a 6 cm fixed-distance from the motor hotspot thus introduced variability in the brain regions and networks targeted with negative consequences, suggesting that future studies might obtain more consistent outcomes if they target using more refined atlases [18,25] and avoid subregion 8Av.

The location of the responder Rlocation relative to the nonresponder Rlocation is consistent with previous work [3] indicating that more anterolateral frontal rTMS targets are more effective. Studies suggest that these targets are associated with more negative functional correlation with the subgenual cingulate and better treatment outcome [7–11]. Although our treated sample was too small for a convincing analysis, our data show a weak correlation between treatment outcome and target connectivity with the subgenual cingulate (eDiscussion: Correlating HAMD change vs. Subgenual Cingulate Connectivity, Figure S3). While we observed that the responder Rlocation was anticorrelated with the subgenual cingulate on average over our 49 participants, individual correlations ranged from 0.49 to 0.18. This result demonstrates that functional connectivity between the same brain regions is widely variable across subjects, suggesting that individualized targeting is necessary when stimulation at a site anticorrelated with subgenual cingulate is the goal. Reliable personalized target identification requires longer resting state acquisitions, preprocessing using global signal regression, little smoothing, a seedmap approach for estimating subgenual cingulate timecourses, and a clustering approach using a high threshold [30].

Prior work showed success when targeting the border of two regions (BA 9 and 46) as a strategy for reaching both [31]. However, if the failure to improve in our active nonresponders was due to inadequate DLPFC modulation despite being targeted at the border of DLPFC and 8Av (see Fig. 1b), this suggests that rTMS does a poor job engaging multiple regions when they are functionally unrelated. Our data also suggest that stimulation of the default mode network may be ineffective at reducing depression severity, at least when the DMN is stimulated via the DLPFC. Our active nonresponder Rlocation is located in area 8Av, evokes the default mode network, and is near a meta-analytically derived depression target that improves anxiosomatic symptoms [14] such as feelings of failure, indecisiveness, irritability, sexual dysfunction, and early and middle insomnia. We cannot rule out the possibility that our active nonresponders had an anxiosomatic pattern of response we were unable to detect. Consistent with the aforementioned metaanalysis [14], the responder Rlocation is close to the target that improves dysphoric symptoms and is functionally connected to the subgenual cingulate. Unfortunately, our small sample precludes a stringent analysis of whether targeting is related to improvement in anxiosomatic vs. dysphoric symptoms (eDiscussion: Response in Relation to Depression Symptoms).

There are several limitations of this study. The major limitation is that the groups stratified by treatment and response are small, ranging from 6 to 15. To address the limited sample size, only the Rlocations were derived using these small samples, and all subjects (N = 49)

were used to estimate group connectomes [32] with the Rlocations. As such, our results reflect group trends and may not generalize to individual patients. Although these Rlocations are still derived from small groups, the low resolution of the original fMRI (3.44 × 3.44 × 3.5 mm) and large radius of the seeds used in our analyses (R = 10 mm) mitigate these concerns to some degree by probing connectivity within a large region surrounding the Rlocation. In essence, the contributions of multiple anatomical regions and networks targeted by the individual stimulation locations are reflected in the group connectome results for each Rlocation. Global signal regression (GSR) was not used in our preprocessing pipeline, even though it was used in prior work reporting DLPFC anticorrelations with subgenual cingulate in depression [8,10,30]. Despite this, we detected a significant average anticorrelation between the active Rlocation and the subgenual cingulate, that may have been stronger with GSR. Also, because stimulation location information was derived from fiducials placed on cloth caps instead of MR-image guidance, our targeting locations were subject to error due to fiducial misplacement or cap movement, and the MNI-coordinates of the location of cortical stimulation cannot account for targeting trajectory. Although the magnitude of these errors is unknown, we expect that localization noise would make it more difficult to detect an effect of stimulation location on outcome and that neuronavigation would strengthen our conclusions. In addition, our seed-based analysis using group centroids as the seeds only approximated the network stimulated by rTMS, while a TMSfMRI study conducting between-group comparisons of responders and nonresponders would be more definitive.

We thus addressed an important concern about the failure to find an advantage of active over sham stimulation in a clinical trial of Veterans undergoing rTMS therapy [16]. Using randomized, carefully blinded, sham-controlled data, we showed that brain stimulation location is related to treatment response in the active and not the sham condition, consistent with previous work [9]. Further study of the active condition revealed that the average focal brain region for responders and not nonresponders has significant anticorrelation with subgenual cingulate, and these average targets evoke different resting-state networks. These results suggest that alternative scalp-targeting rules based on the EEG 10e20 system that adjust for head size [33,34] and more consistently reach DLPFC, or MR-image guidance based on structural MRI [35−37] or potentially fMRI-derived functional connectivity [7] likely would have led to a more successful outcome in CSP556. Our results cannot explain the unusually high placebo response in the original study which deserves further investigation. Since rTMS is FDA approved and widely available, participation in a sham-controlled rTMS study is difficult to justify to treatment-seeking depressed patients. This and other studies demonstrate an alternative method of evaluating rTMS by relating modern brain atlases to imaging and outcomes in clinical rTMS patients. Utilizing these approaches and larger cohorts than sham-controlled studies will enable more powerful statistical analyses of diversity, treatment interactions, and comparisons to real world outcomes, which can potentially be leveraged to create a learning healthcare system [38] for mental illness. Through this approach, clinical targeting could evolve from tracing on the scalp, to targeting based on group atlases, and ultimately to personalized guidance based on multimodal MRI delivered with robotic precision.

Supplementary Material

Refer to Web version on PubMed Central for supplementary material.

Acknowledgments

This work was supported by Cooperative Studies Grant # 556 (DHM, BJR, GHG, BWB, SDF, MSG, MT, DYT, YCS, JAY), and Merit Awards #CX000604 (ACR, JB, AMH) and #RX003152 (ACR, VAC) from the United States (U.S.) Department of Veterans Affairs, Office of Research and Development. PJN, SPD, and MES are employees of Omniscient Neurotechnologies and assisted with blinded data analysis identifying brain subregions underlying fiducial markers. ACR and VAC performed an independent reanalysis, generated Fig. 1, and confirmed these conclusions. Many thanks to Alfonso Nieto-Castanon and Susan Whitfield-Gabrieli for assistance with the CONN toolbox.

Declaration of competing interest

Dr. Rosen, Ms. Bhat, Dr. Cardenas, Dr. Ehrlich, Ms. Horwege, Mr. Roach, Dr. Glover, Dr. Forman, Dr. Yurgelun-Todd, Dr. Scott, Dr. Tian, and Dr. Yesavage have no conflicts to disclose. Dr. Mathalon is a consultant for Boehringer Ingelheim and Caden Therapeutics. Dr. Badran owns a minority stake in Bodhi NeuroTech Inc., which manufactures meditation enhancing devices and holds patents in this area assigned to the Medical University of South Carolina. Dr. George holds research grants through the Medical University of South Carolina with Brainsway and LivaNova. He is on the scientific advisory board, uncompensated, for Magstim, Brainsway. He has equipment loaned from MECTA and Nexstim. He is on the scientific advisory board for Neuralief (compensated). He has no ownership of any brain stimulation device company. He is the editor in chief of Brain Stimulation, published by Elsevier. Dr. Thase reports no conflicts of interest with this research. Dr. Thase reports the following other relationships over the past three years: Advisory/ConsultantdAcadia, Alkermes, Allergan (Forest, Naurex), Axsome, Clexio, Johnson & Johnson (Janssen, Ortho-McNeil), Lundbeck, Merck, Novartis, Otsuka, Pfizer, Shire, Sunovion, Takeda; Grant SupportdAcadia, Allergan (Forest, Naurex), Alkermes, Axsome, Clexio, Myriad (AssureRx), Axsome, Intracellular, Janssen, National Institute of Mental Health, Otsuka, Patient Centered Outcomes Research Institute, Takeda; RoyaltiesdAmerican Psychiatric Press, Guilford Publications, Herald House, W.W. Norton & Company, Inc. Dr. Thases's spouse, Diane Sloan, PharmD, is a Senior Medical Director for Peloton Advantage, which does business with a number of pharmaceutical companies. Dr. Doyen and Dr. Sughrue are directors of Onminscient Neurotechnology Pty. and hold company shares. Dr. Doyen, Dr. Sughrue, and Mr. Nicholas are employees of Omniscient Neurotechnology Pty. Mr. Nicholas holds company employee options in Omniscient Neurotechnology Pty.

References

[1]. Fitzgerald PB, Hoy KE, Anderson RJ, Daskalakis ZJ. A study of the pattern of response to rTMS treatment in depression. Depress Anxiety 2016;33(8): 746–53. [PubMed: 27059158]

[2]. George MS, Taylor JJ, Short EB. The expanding evidence base for rTMS treatment of depression. Curr Opin Psychiatr 2013;26(1):13–8.

[3]. Herbsman T, Avery D, Ramsey D, Holtzheimer P, Wadjik C, Hardaway F, et al. More lateral and anterior prefrontal coil location is associated with better repetitive transcranial magnetic stimulation antidepressant response. Biol Psychiatr 2009;66(5):509–15.

[4]. Johnson KA, Baig M, Ramsey D, Lisanby SH, Avery D, McDonald WM, et al. Prefrontal rTMS for treating depression: location and intensity results from the OPT-TMS multi-site clinical trial. Brain Stimul. 2012;6(2):108–17. [PubMed: 22465743]

[5]. Herwig U, Schonfeldt-Lecuona C, Wunderlich AP, von Tiesenhausen C, Thielscher A, Walter H, et al. The navigation of transcranial magnetic stimulation. Psychiatr Res Neuroimaging 2001;108(2):123–31.

[6]. Padmanabhan JL, Cooke D, Joutsa J, Siddiqi SH, Ferguson M, Darby RR, et al. A human depression circuit derived from focal brain lesions. Biol Psychiatr 2019;86(10):749–58.

[7]. Williams NR, Sudheimer KD, Bentzley BS, Pannu J, Stimpson KH, Duvio D, et al. High-dose spaced theta-burst TMS as a rapid-acting antidepressant in highly refractory depression. Brain 2018;141(3):e18−. [PubMed: 29415152]

[8]. Cash RFH, Zalesky A, Thomson RH, Tian Y, Cocchi L, Fitzgerald PB. Subgenual functional connectivity predicts antidepressant treatment response to transcranial magnetic stimulation:

independent validation and evaluation of personalization. Biol Psychiatr 2019;86(2):e5–7. 10.1016/j.biopsych.2018.12.002.

[9]. Weigand A, Horn A, Caballero R, Cooke D, Stern AP, Taylor SF, et al. Prospective validation that subgenual connectivity predicts antidepressant efficacy of transcranial magnetic stimulation sites. Biol Psychiatr 2018;84(1):28–37.

[10]. Fox MD, Buckner RL, White MP, Greicius MD, Pascual-Leone A. Efficacy of transcranial magnetic stimulation targets for depression is related to intrinsic functional connectivity with the subgenual cingulate. Biol Psychiatr 2012;72(7):595–603.

[11]. Mir-Moghtadaei A, Caballero R, Fried P, Fox MD, Lee K, Giacobbe P, et al. Concordance between BeamF3 and MRI-neuronavigated target sites for repetitive transcranial magnetic stimulation of the left dorsolateral prefrontal cortex. Brain Stimul. 2015;8(5):965–73. [PubMed: 26115776]

[12]. Bestmann S, Baudewig J, Siebner HR, Rothwell JC, Frahm J. Functional MRI of the immediate impact of transcranial magnetic stimulation on cortical and subcortical motor circuits. Eur J Neurosci 2004;19(7):1950–62. [PubMed: 15078569]

[13]. Beynel L, Powers JP, Appelbaum LG. Effects of repetitive transcranial magnetic stimulation on resting-state connectivity: a systematic review. Neuroimage 2020:211.

[14]. Siddiqi SH, Taylor SF, Cooke D, Pascual-Leone A, George MS, Fox MD. Distinct symptom-specific treatment targets for circuit-based neuromodulation. Am J Psychiatr 2020;177(5):435–46. [PubMed: 32160765]

[15]. Mi Z, Biswas K, Fairchild JK, Davis-Karim A, Phibbs CS, Forman SD, et al. Repetitive transcranial magnetic stimulation (rTMS) for treatment-resistant major depression (TRMD) Veteran patients: study protocol for a randomized controlled trial. Trials 2017;18(1):409. [PubMed: 28865495]

[16]. Yesavage JA, Fairchild JK, Mi Z, Biswas K, Davis-Karim A, Phibbs CS, et al. Effect of repetitive transcranial magnetic stimulation on treatment-resistant major depression in US Veterans: a randomized clinical trial. JAMA Psychiatr 2018;75(9):884–93. 10.1001/jamapsychiatry.2018.1483.

[17]. Chow ZR. Sham treatment is as effective for treatment-resistant depression as repetitive transcranial magnetic StimulationSham treatment is as effective for treatment-resistant depression as repetitive transcranial magnetic StimulationLetters. JAMA Psychiatr 2019;76(1):99.

[18]. Glasser MF, Coalson TS, Robinson EC, Hacker CD, Harwell J, Yacoub E. A multimodal parcellation of human cerebral cortex. Nature 2016;536.

[19]. Jenkinson M, Beckmann CF, Behrens TE, Woolrich MW, Smith SM. FSL 15. Neuroimage 2012;62(2):782–90. [PubMed: 21979382]

[20]. Legendre P, Legendre L, Legendre L, Legendre L. Numerical ecology. 2nd English ed. Amsterdam ; New York: Elsevier; 1998.

[21]. Whitfield-Gabrieli S, Nieto-Castanon A. Conn: a functional connectivity toolbox for correlated and anticorrelated brain networks. Brain Connect 2012;2.

[22]. Chai XJ, Castanon AN, Ongur D, Whitfield-Gabrieli S. Anticorrelations in resting state networks without global signal regression. Neuroimage 2012;59(2):1420–8. [PubMed: 21889994]

[23]. Ferri J, Eisendrath SJ, Fryer SL, Gillung E, Roach BJ, Mathalon DH. Blunted amygdala activity is associated with depression severity in treatmentresistant depression. Cognit Affect Behav Neurosci 2017;17(6):1221–31. [PubMed: 29063521]

[24]. Rorden C, Brett M. Stereotaxic display of brain lesions. Behav Neurol 2000;12(4):191–200. [PubMed: 11568431]

[25]. Yeo BTT, Krienen FM, Sepulcre J, Sabuncu MR, Lashkari D, Hollinshead M, et al. The organization of the human cerebral cortex estimated by intrinsic functional connectivity. J Neurophysiol 2011;106(3):1125–65. [PubMed: 21653723]

[26]. Schaefer A, Kong R, Gordon EM, Laumann TO, Zuo XN, Holmes AJ, et al. Localglobal parcellation of the human cerebral cortex from intrinsic functional connectivity MRI. Cerebr Cortex 2018;28(9):3095–114.

[27]. Zou KH, Warfield SK, Bharatha A, Tempany CM, Kaus MR, Haker SJ, et al. Statistical validation of image segmentation quality based on a spatial overlap index. Acad Radiol 2004;11(2):178–89. [PubMed: 14974593]

[28]. Dosenbach NU, Fair DA, Cohen AL, Schlaggar BL, Petersen SE. A dual-networks architecture of top-down control. Trends Cognit Sci 2008;12(3):99–105. [PubMed: 18262825]

[29]. Raichle ME, MacLeod AM, Snyder AZ, Powers WJ, Gusnard DA, Shulman GL. A default mode of brain function. Proc Natl Acad Sci U S A 2001;98(2):676–82. [PubMed: 11209064]

[30]. Cash RFH, Cocchi L, Lv J, Wu Y, Fitzgerald PB, Zalesky A. Personalized connectivity-guided DLPFC-TMS for depression: advancing computational feasibility, precision and reproducibility. Hum Brain Mapp 2021. 10.1002/hbm.25330.

[31]. Fitzgerald PB, Hoy K, McQueen S, Maller JJ, Herring S, Segrave R, et al. A randomized trial of rTMS targeted with MRI based neuro-navigation in treatment-resistant depression. Neuropsychopharmacology 2009;34(5): 1255–62. [PubMed: 19145228]

[32]. Nauczyciel C, Hellier P, Morandi X, Blestel S, Drapier D, Ferre JC, et al. Assessment of standard coil positioning in transcranial magnetic stimulation in depression. Psychiatr Res 2011;186(2−3):232–8.

[33]. Beam W, Borckardt JJ. Beam F3 locator program. http://www.clinicalresearcher.org/software.htm; 2010.

[34]. Beam W, Borckardt JJ, Reeves ST, George MS. An efficient and accurate new method for locating the F3 position for prefrontal TMS applications. Brain Stimul. 2009;2(1):50–4. [PubMed: 20539835]

[35]. Peleman K, Van Schuerbeek P, Luypaert R, Stadnik T, De Raedt R, De Mey J, et al. Using 3D-MRI to localize the dorsolateral prefrontal cortex in TMS research. World J Biol Psychiatr 2010;11(2−2):425–30.

[36]. Baeken C, Marinazzo D, Wu G-R, Van Schuerbeek P, De Mey J, Marchetti I, et al. Accelerated HF-rTMS in treatment-resistant unipolar depression: insights from subgenual anterior cingulate functional connectivity. World J Biol Psychiatr 2014;15(4):286–97.

[37]. Mylius V, Ayache SS, Ahdab R, Farhat WH, Zouari HG, Belke M, et al. Definition of DLPFC and M-1 according to anatomical landmarks for navigated brain stimulation: inter-rater reliability, accuracy, and influence of gender and age. Neuroimage 2013;78:224–32. [PubMed: 23567888]

[38]. Olsen L, Aisner D, McGinnis M. The learning healthcare system: workshop summary (IOM roundtable on evidence-based medicine). Washington, D.C.: National Academies Press; 2007.

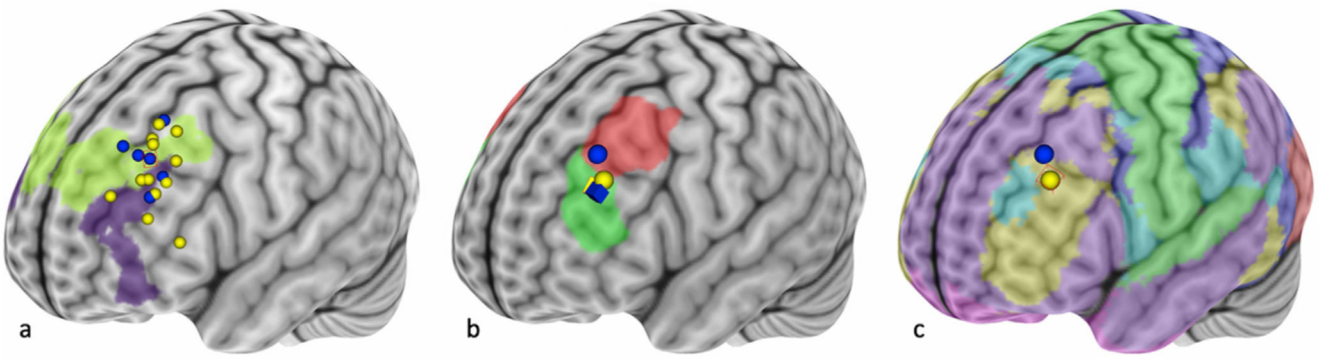

Fig. 1.

a) Individual active stimulation locations with nonresponders in blue and responders in yellow with traditional BA 9/46 overlaid in green/purple. **b**) Derived Rlocations. Blue: nonresponders, yellow: reponders, squares: sham, circles: active. The human connectome maps for DLPFC/8Av are overlaid in green/red. **c**) Active responder and nonresponder Rlocations with the Yeo 7-network map overlaid, showing the nonresponders in a default mode network and the responders in a frontoparietal network. (For interpretation of the references to colour in this figure legend, the reader is referred to the Web version of this article.)

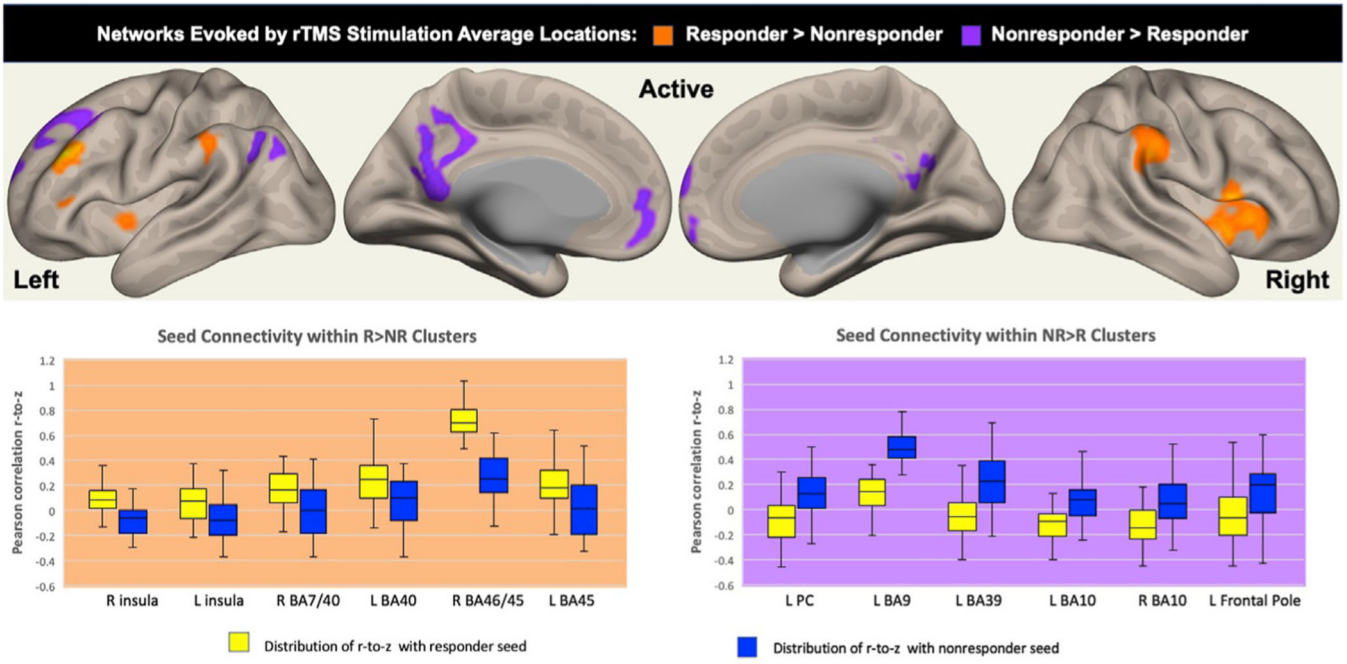

Fig. 2.

Networks functionally connected to the brain regions underlying the active-responder and active-nonresponder scalp targets are compared. Yellow/orange denotes regions more connected to the responder location and purple denotes regions more connected to the nonresponder location. Box-and-whisker plots showing the average correlation with each seed for each cluster listed in Table 3 are also shown. (For interpretation of the references to colour in this figure legend, the reader is referred to the Web version of this article.)

Table 1

Demographic information.

Variable	All (N = 49) Mean (SD) or n (%)	Original Study (N = 164) Mean (SD) or n (%)
Age	56.0(11.9)	55.2 (12.4)
Male	39 (79.6%)	132 (80.5%)
Education above high school (N = 42)	24 (57.1%)	89 (54.3%)
Caucasian (N = 44)	40 (81.6%)	126(77.3%)
HAMD24	26.4 (4.6)	26.9 (5.0)
BDI-II score (N = 45)[a]	23.3 (10.26)	24.5 (10.3)
PTSD (PCL-M) (N = 45)[a]	42.7 (17.3)	42.8 (18.1)

[a]These measures were collected at the time of imaging; all others are baseline values.

Table 2

Atlas labeling at rlocations.

	Traditional atlas	HCP parcellation	Yeo-7 parcellation	Yeo-17/Schaefer parcellation
Active nonresponder	BA 9	8Av	Default mode	Default mode-A
Active responder	BA 46	46	Frontoparietal	Salience/Ventral Attention A
Sham nonresponder	BA 46	46	Frontoparietal	Salience/Ventral Attention A
Sham responder	BA 46	46	Frontoparietal	Salience/Ventral Attention A

Table 3

Differences in networks functionally connected to the brain regions underlying active-responder and active-nonresponder scalp targets. MNI coordinates are reported for each brain region that served as the seed voxel. Within each cluster, the increase in average correlation (z-score) with the responder seed compared to the nonresponder seed is estimated by β; a negative b denotes the cluster is more strongly correlated to the nonresponder seed.

Descriptor	Side	Volume (mm^3)	cluster size p FDR corrected	Change in mean r-to-z	Peak		
					x	y	z
Responder (−42, 34, 38) > Nonresponder (−34, 30, 46)							
Insula							
Insula/Inferior Frontal/Temporal Pole	R	1043	0	0.25	54	10	6
Insula	L	79	0.0182	0.20	−46	0	−2
Parietal/Posterior Cingulate/Supramarginal Gyrus *BA 7/40	R	742	0	0.28	50	−42	60
BA 40	L	171	0.0005	0.26	−60	−30	44
Prefrontal							
*Dorsolateral/Ventrolateral PFC (BA 46/BA 45)	L	466	0	0.43	−40	34	34
Ventrolateral PFC (BA 45)	L	66	0.0303	0.26	−52	36	8
Nonresponder (−34, 30, 46) > Responder (−42, 34, 38)							
Posterior cingulate	L	984	0	−0.33	−4	−40	40
Middle/Superior Frontal Gyrus (BA 9)	L	750	0	−0.39	−30	30	48
L. Occipital/Angular Gyrus (BA 39)	L	286	0	−0.32	−50	−68	38
Ventral Frontal Regions							
Paracingulate Gyrus, Medial Frontal Cortex (BA 10)	L	240	0.0001	−0.30	−2	48	−8
Frontal Pole (BA 10)	R	155	0.0008	−0.28	2	62	16
Frontal Pole, Paracingulate Gyrus (BA 10)	L	78	0.0182	−0.26	−16	58	24